Journal of Molecular Structure (Theochem), 188 (1989) 15-43
Elsevier Science Publishers B.V., Amsterdam — Printed in The Netherlands

AB INITIO FORCE FIELDS OF ALANINE DIPEPTIDE IN C_5 AND C_7 CONFORMATIONS

T.C. CHEAM and S. KRIMM

Biophysics Research Division and Department of Physics, University of Michigan, Ann Arbor, MI 48109 (U.S.A.)

(Received 26 August 1988)

ABSTRACT

We have followed up our previous ab initio calculations of the force fields and dipole-moment derivatives of glycine dipeptide in C_5 and C_7 conformations with similar studies of the L-alanyl compound [$CH_3CONHCH(CH_3)CONHCH_3$]. We have done, with the 4-21 Gaussian basis set, calculations of the three lowest-energy optimized conformations with intramolecular hydrogen bonding that were derived by Scarsdale et al.: the C_5, C_7^{eq}, and C_7^{ax} structures. The quadratic force constants were scaled, as in our previous work, using the set of scale factors derived by Fogarasi and Balázs for small amides, with slight modifications. The differences in the force constants, harmonic frequencies, dipole derivatives, and infrared intensities among the conformations and within each conformation are discussed and related, where possible, to differences in hydrogen bonding and structure. The results are also compared and integrated with those on Gly dipeptide. The force constants and dipole derivatives show that the C_7^{ax} hydrogen bond is the strongest, in agreement with the NH···O geometries, even though the SCF energy of this conformer is the highest. The NH stretch and the amide **I** and **II** modes are compared with available infrared data on Ala dipeptide in argon matrix, and the comparison supports the empirically based conclusion that C_5 and C_7 conformations are both present in the matrix-isolated sample. The problem of distinguishing between the C_7^{eq} and C_7^{ax} forms is also discussed.

INTRODUCTION

We have previously [1] given the results of ab initio calculations of the force fields and dipole-moment derivatives of glycine dipeptide in the C_5 and C_7 conformations with intramolecular hydrogen bonding [2]. We now report on similar studies of the L-alanyl compound, $CH_3CONHCH(CH_3)CONHCH_3$, in the three lowest-energy conformations derived by Scarsdale et al. [3] with the 4-21 basis set: the C_5, C_7^{eq}, and C_7^{ax} structures.

From empirical vibrational analyses of polypeptides [4], it has been found that some of the normal modes of the amide group involve significant displacements at the C^{α} atom. The Ala dipeptide is, therefore, a more representative model than Gly dipeptide for studying the modes of polypeptides and proteins.

In the following, after giving some details of the calculations, we discuss the

0166-1280/89/$03.50

force fields, normal modes and dipole derivatives, and then compare them with some available experimental data. Throughout, the results are compared and integrated with those on Gly.

METHOD OF CALCULATION

The three Ala dipeptide conformations are shown in Fig. 1. The cartesian axes and atomic coordinates are as given by Scarsdale et al. [3] (our numbering of the terminal H atoms corresponds to their Table 1, but not to their Fig. 2). The dihedral angles [5] (ϕ, ψ) have the values ($-165.7°$, $167.3°$) in the C_5, ($-84.6°$, $73.0°$) in the C_7^{eq}, and ($74.6°$, $-62.0°$) in the C_7^{ax} conformations. In the C_5 conformation (ALA5), an intramolecular five-membered NH···OC

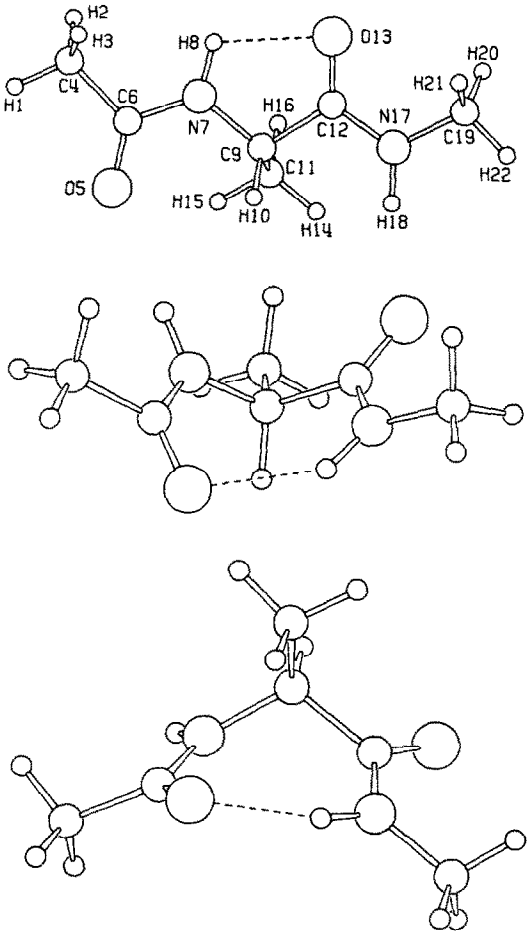

Fig. 1. Alanine dipeptide conformations. Top to bottom: C_5, C_7^{eq}, and C_7^{ax}.

TABLE 1

Internal coordinates for alanine dipeptide

R	Atoms	ALA5[a]	ALA7E[a]	ALA7A[a]	R	Atoms	ALA5[a]	ALA7E[a]	ALA7A[a]
Bond stretches (Å)					*Angle bends (°) (cont.)*				
1	4- 6	1.518	1.517	1.519	37	1- 4- 2	109.6	109.7	109.4
2	6- 7	1.353	1.353	1.353	38	1- 4- 3	109.7	109.5	109.7
3	7- 9	1.453	1.473	1.478	39	2- 4- 3	108.4	108.6	108.6
4	6- 5	1.226	1.230	1.231	40	7- 9-12	106.4	109.5	112.7
5	7- 8	0.997	0.995	0.994	41	7- 9-10	109.3	106.8	106.0
6	9-12	1.528	1.539	1.538	42	12- 9-10	109.8	108.6	104.2
7	12-17	1.348	1.346	1.343	43	11- 9-10	109.3	111.1	109.1
8	17-19	1.466	1.462	1.462	44	7- 9-11	111.6	110.1	112.5
9	12-13	1.227	1.225	1.226	45	12- 9-11	110.5	110.7	111.8
10	17-18	0.993	0.998	0.998	46	9-11-14	111.3	109.9	109.4
11	4- 1	1.077	1.077	1.077	47	9-11-15	108.2	110.1	109.5
12	4- 2	1.083	1.082	1.083	48	9-11-16	109.7	110.1	110.9
13	4- 3	1.083	1.083	1.082	49	14-11-15	109.1	109.1	108.7
14	9-11	1.545	1.528	1.540	50	14-11-16	109.0	107.5	109.5
15	9-10	1.081	1.079	1.077	51	15-11-16	109.5	110.0	108.9
16	11-14	1.083	1.080	1.082	52	17-19-20	110.4	110.3	111.0
17	11-15	1.079	1.082	1.082	53	17-19-21	110.4	111.1	110.5
18	11-16	1.082	1.081	1.076	54	17-19-22	108.7	108.6	108.6
19	19-20	1.080	1.081	1.082	55	20-19-21	108.5	108.2	108.2
20	19-21	1.080	1.082	1.081	56	20-19-22	109.4	109.3	109.3
21	19-22	1.079	1.079	1.080	57	21-19-22	109.4	109.3	109.3
Angle bends (°)									
22	4- 6- 7	114.7	115.2	114.6					
23	4- 6- 5	123.2	122.8	121.9	*Out-of-plane bends[b] (°)*				
24	7- 6- 5	122.1	122.0	123.5	58	6- 5	−0.1	−0.1	0.3
25	6- 7- 9	121.3	121.9	125.9	59	7- 8	1.6	1.4	−1.3
26	6- 7- 8	123.2	120.3	118.0	60	12-13	−1.1	0.4	1.4
27	9- 7- 8	115.5	117.8	116.1	61	17-18	−1.3	−5.3	3.8
28	9-12-17	115.7	114.2	116.1					
29	9-12-13	121.7	122.1	120.3	*Torsions*				
30	17-12-13	122.6	123.6	123.6	62	4- 6			
31	12-17-19	120.3	120.3	119.9	63	6- 7			
32	12-17-18	120.4	118.9	119.4	64	7- 9			
33	19-17-18	119.3	120.6	120.6	65	9-12			
34	6- 4- 1	108.7	108.6	108.5	66	12-17			
35	6- 4- 2	110.2	110.4	110.1	67	17-19			
36	6- 4- 3	110.3	110.1	110.4	68	9-11			

[a]Equilibrium values. [b]Positive: C6, N17 move out of ALA5 plane in Fig. 1; N7, C12 move below plane.

TABLE 2

Group coordinates for alanine dipeptide[a]

$S_1 = R_5$	NH str1	$S_{31} = 2R_{39} - R_{37} - R_{38}$	M1 ab1
$S_2 = R_4$	CO str1	$S_{32} = R_{37} - R_{38}$	M1 ab2
$S_3 = R_2$	CN str1	$S_{33} = 2R_{34} - R_{35} - R_{36}$	M1 rock1
$S_4 = R_1$	MC str	$S_{34} = R_{35} - R_{36}$	M1 rock2
$S_5 = R_3$	NC^{α} str	$S_{35} = R_{40} + R_{44} + R_{45} - R_{41} - R_{42} - R_{43}$	$NC^{\alpha}C$ def
$S_6 = R_{10}$	NH str2	$S_{36} = 2R_{43} - R_{41} - R_{42}$	H^{α} b1
$S_7 = R_9$	CO str2	$S_{37} = R_{41} - R_{42}$	H^{α} b2
$S_8 = R_7$	CN str2	$S_{38} = 2R_{40} - R_{44} - R_{45}$	C^{β} b1
$S_9 = R_6$	$C^{\alpha}C$ str	$S_{39} = R_{44} - R_{45}$	C^{β} b2
$S_{10} = R_8$	NM str	$S_{40} = R_{49} + R_{50} + R_{51} - R_{46} - R_{47} - R_{48}$	C^{β} sb
$S_{11} = R_{11}$	MH1 str	$S_{41} = 2R_{49} - R_{50} - R_{51}$	C^{β} ab1
$S_{12} = R_{12}$	MH2 str	$S_{42} = R_{50} - R_{51}$	C^{β} ab2
$S_{13} = R_{13}$	MH3 str	$S_{43} = 2R_{48} - R_{46} - R_{47}$	C^{β} rock1
$S_{14} = R_{14}$	$C^{\alpha}C^{\beta}$ str	$S_{44} = R_{46} - R_{47}$	C^{β} rock2
$S_{15} = R_{15}$	$C^{\alpha}H^{\alpha}$ str	$S_{45} = R_{55} + R_{56} + R_{57} - R_{52} - R_{53} - R_{54}$	M2 sb
$S_{16} = R_{18}$	CH16 str	$S_{46} = 2R_{55} - R_{56} - R_{57}$	M2 ab1
$S_{17} = R_{16}$	CH14 str	$S_{47} = R_{56} - R_{57}$	M2 ab2
$S_{18} = R_{17}$	CH15 str	$S_{48} = 2R_{54} - R_{52} - R_{53}$	M2 rock1
$S_{19} = R_{21}$	MH22 str	$S_{49} = R_{52} - R_{53}$	M2 rock2
$S_{20} = R_{19}$	MH20 str	$S_{50} = R_{58} \sin(4-6-7)$	CO ob1
$S_{21} = R_{20}$	MH21 str	$S_{51} = R_{59} \sin(6-7-9)$	NH ob1
$S_{22} = 2R_{22} - R_{23} - R_{24}$	MCN def	$S_{52} = R_{60} \sin(9-12-17)$	CO ob2
$S_{23} = R_{23} - R_{24}$	CO ib1	$S_{53} = R_{61} \sin(12-17-19)$	NH ob2
$S_{24} = 2R_{25} - R_{26} - R_{27}$	CNC^{α} def	$S_{54} = R_{62}$	MC tor
$S_{25} = R_{26} - R_{27}$	NH ib1	$S_{55} = R_{63}$	CN tor1
$S_{26} = 2R_{28} - R_{29} - R_{30}$	$C^{\alpha}CN$ def	$S_{56} = R_{64}$	NC^{α} tor
$S_{27} = R_{29} - R_{30}$	CO ib2	$S_{57} = R_{65}$	$C^{\alpha}C$ tor
$S_{28} = 2R_{31} - R_{32} - R_{33}$	CNM def	$S_{58} = R_{66}$	CN tor2
$S_{29} = R_{32} - R_{33}$	NH ib2	$S_{59} = R_{67}$	NM tor
$S_{30} = R_{37} + R_{38} + R_{39} - R_{34} - R_{35} - R_{36}$	M1 sb	$S_{60} = R_{68}$	$C^{\alpha}C^{\beta}$ tor

[a]All coordinates normalized. Normalization factors not shown for $S_{22} - S_{49}$.

hydrogen-bonded ring is present, whereas the C_7 conformations have seven-membered hydrogen-bonded rings, with the methyl side chain equatorial (ALA7E) or axial (ALA7A) to the ring (Fig. 1). None of the conformations has any symmetry, and ALA5 and ALA7A resemble, respectively, the C_5 (GLY5) and C_7 (GLY7) conformations of Gly dipeptide that we studied previously [1].

The primitive internal coordinates and the equilibrium molecular dimensions are given in Table 1, and Table 2 lists the group, or local symmetry, coordinates $\vec{S}$. The quadratic and semi-diagonal cubic force constants and dipole-moment derivatives were computed with the 4-21 Gaussian basis [6] as in [1], using two-sided displacements along $\vec{S}$. The force constants were scaled

using the set of scale factors derived by Fogarasi and Balaźs [7] for some amides, which we modified slightly for Gly dipeptide. For the new group coordinates at the C^{α} atom in Ala dipeptide, the scale factors used were: S_{35}, S_{38} and S_{39}, 0.80; and S_{36} and S_{37}, 0.76. Note that S_{35} ($NC^{\alpha}C$ def) is defined differently than in Gly dipeptide.

FORCE FIELDS AND FREQUENCIES

Table 3 gives the scaled off-diagonal force constants in the group coordinate basis for ALA5, ALA7E and ALA7A; for brevity we list only terms with magnitude $\geqslant 0.05$ in at least one of the conformations; terms of magnitude smaller than 0.01 are shown as 0.0. In Table 4 we list the scaled diagonal force constants together with the equivalent ones of GLY5 and GLY7 for comparison. Finally, Table 5 shows the harmonic frequencies for the Ala dipeptides computed with all scaled $|F_{ij}| \geqslant 0.01$.

First, we will discuss the force constants. In Gly dipeptide we were able to relate many of the force constants of the CONH groups to the C_5 and C_7 hydrogen bonds. Similar results are seen in Ala dipeptide. Thus, the hydrogen-bonded NH stretch (str) and CO str terms are smaller than the free. The differences between the bonded and free f(NH str) and f(CO str) are largest in ALA7A, indicating that the C_7^{ax} hydrogen bond is the strongest. This is consistent with the NH and CO bond lengths (Table 1) and with the H···O distances of 2.13 Å, 2.07 Å and 1.94 Å, and the NH···O angles of 108°, 141° and 147° in ALA5, ALA7E and ALA7A, respectively. (For reference, in GLY5 and GLY7 the H···O distances are 2.17 Å and 2.06 Å, and the NH···O angles are 108° and 142°.) Note, however, that the 4-21 SCF energy of ALA7A is in fact the highest [2]: 2.6 kcal mol^{-1} above that of ALA7E and 1.2 kcal mol^{-1} above that of ALA5. The geometry and force constants of the NH···OC group (and also the NH str dipole moment derivative) are more direct measures of the hydrogen-bond strength than is the energy, which depends on total intra- and inter-molecular interaction and which in general cannot be uniquely partitioned to yield a purely hydrogen-bond component.

The CO in-plane (ib) and out-of-plane (ob) bend force constants also show the effects of the C_5 and C_7 hydrogen bonds, being higher for the bonded CO group in each structure. As in Gly dipeptide, the NH ib force constant shows the expected trend in the C_7 structues, whereas in ALA5 the bonded f(NH ib1) is less than f(NH ib2). In the C_5 structures the differences between the angles $C_6N_7H_8$ and $C_9N_7H_8$ are by far the largest, 7.7° (ALA5) and 7.9° (GLY5), and this may be related to the lowered f(NH ib1). The free f(NH ib) is 0.59 mdyne Å rad^{-2} in all structures except ALA7A, where its magnitude is 0.61; significantly, the angle $C_6N_7C_9$ is very much the largest in ALA7A. A plausible conclusion, then, is that f(NH ib) decreases when the difference between the angles adjacent to the NH bond increases, and it increases when the opposite

TABLE 3

Scaled off-diagonal force constants, $|F_{ij}| \geq 0.05$[a]

Term	ALA5	ALA7E	ALA7A	Term	ALA5	ALA7E	ALA7A	Term	ALA5	ALA7E	ALA7A
1- 5	0.13	0.04	0.0	6-57	0.01	0.05	−0.04	13-32	−0.09	−0.10	−0.10
1- 7	−0.10	−0.01	0.0	7- 8	1.31	1.30	1.28	13-33	−0.05	−0.05	−0.05
1- 8	0.05	0.0	0.0	7- 9	0.41	0.37	0.40	13-34	−0.09	−0.09	−0.09
1- 9	−0.06	0.0	−0.02	7-10	−0.08	−0.07	−0.07	14-24	0.02	0.04	0.06
1-22	0.0	−0.01	−0.05	7-25	−0.06	−0.01	0.0	14-26	0.02	0.08	0.02
1-24	−0.11	−0.09	−0.08	7-26	−0.54	−0.47	−0.47	14-35	0.10	0.15	0.16
1-25	−0.11	0.02	0.04	7-27	−0.05	−0.09	−0.09	14-36	0.23	0.20	0.22
2- 3	1.37	1.36	1.30	7-35	0.03	−0.02	0.12	14-38	−0.25	−0.26	−0.24
2- 4	0.36	0.36	0.38	7-37	−0.04	−0.07	0.0	14-39	−0.07	−0.07	−0.02
2- 5	−0.09	−0.09	−0.09	7-38	0.03	0.10	0.08	14-40	−0.33	−0.33	−0.35
2- 6	0.0	−0.14	−0.17	7-39	−0.04	0.0	−0.08	15-24	−0.05	−0.07	0.0
2- 8	0.0	0.05	0.06	7-55	0.0	−0.05	0.05	15-26	−0.04	−0.05	0.07
2-22	−0.55	−0.55	−0.49	7-56	0.0	−0.06	0.06	15-27	0.02	0.02	−0.06
2-23	−0.16	−0.14	−0.05	8- 9	0.24	0.23	0.19	15-35	−0.12	−0.12	−0.11
2-26	−0.02	0.08	0.07	8-10	0.10	0.11	0.11	16-24	0.0	0.0	−0.09
2-27	0.05	0.05	0.06	8-22	0.0	0.04	0.06	16-35	−0.04	−0.06	−0.12
2-35	0.03	−0.02	0.08	8-23	0.0	0.05	0.08	16-38	0.01	0.02	0.05
2-38	0.04	0.07	0.03	8-24	0.03	−0.05	−0.09	16-40	0.06	0.06	0.06
2-39	0.05	0.0	0.03	8-26	0.18	0.14	0.08	16-41	−0.11	−0.11	−0.09
3- 4	0.31	0.30	0.31	8-27	−0.45	−0.42	−0.42	16-43	0.08	0.09	0.06
3- 5	0.20	0.24	0.30	8-28	0.18	0.15	0.17	16-56	0.0	0.0	0.08
3- 8	−0.03	−0.09	−0.11	8-29	0.19	0.25	0.26	17-39	0.08	0.05	0.04
3- 9	−0.03	0.04	0.07	8-35	−0.02	0.05	−0.10	17-40	0.07	0.06	0.05
3-15	−0.04	−0.05	−0.02	8-36	0.0	0.0	−0.06	17-41	0.06	0.05	0.10
3-22	0.19	0.16	0.17	8-37	−0.04	0.0	−0.07	17-42	0.10	0.10	0.05
3-23	−0.45	−0.50	−0.49	8-39	−0.05	−0.08	0.0	17-43	−0.04	−0.05	−0.05
3-24	0.21	0.22	0.23	8-48	0.07	0.07	0.08	17-44	0.07	0.08	0.09
3-25	0.17	0.19	0.22	8-50	0.0	−0.06	0.07	18-39	−0.07	−0.05	−0.04
3-26	0.0	0.03	0.06	8-53	0.01	0.08	−0.06	18-40	0.05	0.06	0.07
3-29	0.0	−0.05	−0.05	8-55	0.0	0.10	−0.11	18-41	0.05	0.05	0.05
3-35	−0.02	−0.02	0.19	8-56	−0.01	0.13	−0.17	18-42	−0.08	−0.09	−0.10
3-37	−0.05	−0.05	0.03	9-14	0.19	0.18	0.17	18-44	−0.07	−0.08	−0.07
3-51	0.0	−0.07	0.06	9-16	0.0	−0.06	0.0	19-45	0.06	0.06	0.06
3-55	0.01	−0.07	0.09	9-23	−0.02	−0.08	−0.13	19-46	−0.12	−0.12	−0.12
3-56	0.02	−0.06	0.06	9-24	0.0	0.18	0.29	19-48	0.08	0.08	0.08
4-22	0.21	0.21	0.21	9-26	0.11	0.36	0.46	20-45	0.06	0.06	0.06
4-30	0.25	0.25	0.26	9-27	0.43	0.29	0.22	20-46	0.06	0.06	0.07
4-23	−0.29	−0.30	−0.30	9-29	0.02	0.04	0.06	20-47	0.10	0.10	0.10
5- 7	0.05	0.10	0.10	9-35	0.28	0.10	0.40	20-49	0.05	0.05	0.05
5- 8	−0.03	0.07	0.05	9-36	−0.10	−0.19	−0.05	21-45	0.06	0.06	0.06
5- 9	0.17	0.32	0.38	9-37	−0.18	−0.19	−0.17	21-46	0.06	0.07	0.06
5-14	0.25	0.16	0.25	9-38	0.47	0.19	0.23	21-47	−0.10	−0.10	−0.10
5-15	0.11	0.08	0.03	9-39	−0.20	−0.31	−0.18	21-49	−0.05	−0.05	−0.05
5-22	0.02	−0.03	−0.08	9-50	0.0	0.06	−0.06	22-23	0.16	0.19	0.20
5-23	0.06	0.0	−0.13	9-51	0.0	−0.10	0.13	22-24	0.04	−0.02	−0.09
5-24	0.26	0.42	0.60	9-52	0.0	−0.05	0.05	22-26	0.02	−0.03	−0.06
5-25	−0.18	−0.18	−0.20	9-55	0.0	−0.11	0.12	22-33	0.12	0.12	0.11
5-26	0.11	0.11	0.20	9-56	−0.03	−0.24	0.27	22-35	0.01	0.05	−0.19
5-27	−0.10	0.04	0.07	9-57	−0.06	0.06	−0.05	22-38	0.02	−0.06	−0.02
5-35	0.17	0.06	0.67	10-20	0.10	0.11	0.13	23-24	−0.04	−0.16	−0.29
5-36	−0.16	−0.24	−0.09	10-21	0.10	0.13	0.11	23-25	−0.05	−0.05	−0.05
5-37	0.31	0.31	0.29	10-26	0.07	0.07	0.07	23-26	0.01	−0.09	−0.14
5-38	0.21	0.46	0.32	10-27	0.10	0.10	0.10	23-33	−0.09	−0.08	−0.08
5-39	0.38	0.30	0.35	10-28	0.21	0.23	0.24	23-35	0.01	0.08	−0.36
5-43	−0.05	−0.04	0.0	10-29	−0.18	−0.18	−0.19	23-36	0.0	0.04	−0.05
5-44	0.07	0.07	0.06	10-45	−0.51	−0.50	−0.50	23-38	0.02	−0.15	−0.08

TABLE 3 (continued)

Term	ALA5	ALA7E	ALA7A	Term	ALA5	ALA7E	ALA7A	Term	ALA5	ALA7E	ALA7A
5-51	0.0	−0.07	0.08	11-22	0.06	0.06	0.06	23-51	−0.02	0.06	−0.07
5-53	0.0	0.05	−0.06	11-23	−0.05	−0.05	−0.05	23-55	−0.02	0.06	−0.05
5-56	0.07	−0.19	0.16	11-31	−0.10	−0.10	−0.09	23-56	−0.04	0.13	−0.13
5-57	0.04	0.17	−0.19	11-33	0.10	0.10	0.10	23-57	0.0	−0.05	0.06
5-58	0.0	0.09	−0.10	12-30	0.05	0.06	0.05	24-26	0.04	0.20	0.35
6- 8	−0.01	0.05	0.07	12-31	0.06	0.05	0.06	24-28	−0.01	−0.03	−0.05
6-10	−0.07	−0.05	−0.03	12-32	0.10	0.09	0.10	24-35	−0.02	−0.12	0.78
6-26	−0.05	0.05	0.05	12-33	−0.05	−0.05	−0.05	24-36	0.02	−0.10	0.10
6-28	−0.09	−0.07	−0.06	12-34	0.09	0.09	0.09	24-38	−0.05	0.33	0.21
6-29	0.04	0.11	0.12	13-30	0.06	0.05	0.06	24-39	0.09	0.04	0.08
6-53	0.01	0.06	−0.04	13-31	0.06	0.06	0.05	24-43	0.0	0.0	0.06
24-51	0.03	−0.11	0.12	36-43	0.07	0.07	0.06				
24-52	0.02	−0.06	0.08	36-51	0.04	0.04	0.06				
24-53	0.0	0.07	−0.10	36-55	0.0	0.05	0.08				
24-55	0.03	−0.06	0.04	36-56	0.05	0.14	0.18				
24-56	0.07	−0.22	0.21	36-57	−0.05	−0.06	−0.09				
24-57	0.03	0.24	−0.31	37-55	0.03	0.05	0.07				
24-58	0.02	0.08	−0.11	37-56	0.11	0.06	0.12				
26-27	0.02	0.04	0.06	37-57	0.05	0.09	0.09				
26-29	−0.01	0.05	0.07	37-58	0.0	0.05	0.05				
26-35	0.0	−0.04	0.40	38-39	−0.06	0.03	−0.14				
26-36	0.04	−0.08	0.04	38-43	0.06	0.04	0.02				
26-37	0.0	0.0	−0.06	38-50	−0.01	0.06	−0.08				
26-38	0.0	0.23	0.21	38-51	−0.05	−0.20	0.22				
26-39	−0.06	−0.02	−0.03	38-55	0.0	−0.08	0.10				
26-50	0.0	0.07	−0.09	38-56	−0.05	−0.36	0.34				
26-51	0.0	−0.11	0.15	38-57	0.02	0.17	−0.17				
26-55	−0.01	−0.10	0.12	39-44	0.10	0.11	0.12				
26-56	−0.02	−0.26	0.34	39-50	0.0	0.04	0.05				
26-57	−0.01	0.05	−0.09	39-51	0.07	0.0	−0.08				
27-28	0.04	0.05	0.05	39-55	0.0	−0.05	−0.10				
27-29	−0.06	−0.06	−0.06	39-56	0.01	−0.07	−0.16				
27-35	0.09	0.06	0.0	39-57	0.02	−0.08	−0.12				
27-38	0.16	−0.05	0.02	39-58	0.01	−0.04	−0.06				
27-39	−0.02	−0.07	−0.04	49-59	0.05	0.05	0.05				
27-56	0.0	0.06	−0.06	50-51	−0.05	−0.08	−0.13				
28-29	−0.02	−0.07	−0.08	50-55	−0.08	−0.14	−0.15				
28-35	0.03	0.04	−0.12	50-56	−0.10	−0.18	−0.24				
28-38	0.05	−0.07	−0.05	50-57	0.0	−0.05	−0.07				
28-56	0.01	0.06	−0.07	51-55	−0.08	−0.02	0.05				
29-35	0.0	0.0	0.07	51-56	0.0	0.16	0.25				
34-50	0.08	0.08	0.08	51-57	−0.10	−0.02	−0.02				
35-36	0.03	0.07	0.18	52-53	−0.07	−0.07	−0.09				
35-37	−0.06	−0.05	−0.04	52-55	0.02	−0.06	−0.05				
35-38	0.27	−0.19	0.31	52-56	0.10	0.02	0.02				
35-39	0.06	−0.06	0.04	52-57	−0.01	−0.08	−0.10				
35-43	−0.08	−0.06	−0.02	53-55	0.02	0.08	0.09				
35-50	0.0	−0.03	−0.08	53-56	−0.02	0.07	0.09				
35-51	0.03	0.01	0.19	53-57	0.06	0.15	0.19				
35-52	−0.03	0.05	0.08	53-58	−0.09	0.0	0.0				
35-53	−0.02	−0.02	−0.05	55-56	0.13	0.29	0.39				
35-55	0.0	0.07	0.11	55-57	0.09	0.08	0.09				
35-56	0.0	0.15	0.38	56-57	0.10	0.05	0.06				
35-57	−0.08	−0.04	−0.21	56-58	0.04	0.06	0.06				
35-58	0.0	−0.05	−0.05	57-58	0.03	0.17	0.24				
36-38	−0.03	−0.14	0.11								

[a]Units: energy in mdyn Å; stretching coordinates in Å; bending coordinates in radians.

TABLE 4

Scaled diagonal force constants of Ala and Gly dipeptides[a]

	ALA5	ALA7E	ALA7A	GLY5	GLY7
NH str1	6.363	6.453	6.577	6.397	6.523
CO str1	11.040	10.652	10.550	11.167	10.720
CN str1	6.661	6.635	6.631	6.607	6.636
MC str	4.170	4.187	4.167	4.186	4.200
NC^{α} str	5.168	4.856	4.922	5.356	5.081
NH str2	6.666	6.239	6.134	6.511	6.246
CO str2	10.922	11.026	10.965	10.983	11.262
CN str2	6.794	6.901	7.032	6.773	6.937
$C^{\alpha}C$ str	4.259	4.126	4.039	4.293	4.055
NM str	5.206	5.289	5.282	5.204	5.290
MH1 str	4.971	4.982	4.991	4.973	4.986
MH2 str	4.796	4.804	4.785	4.798	4.792
MH3 str	4.797	4.789	4.805	4.798	4.810
$C^{\alpha}C^{\beta}$ str	4.088	4.373	4.131		
$C^{\alpha}H^{\alpha}$ str	4.801	4.918	4.941	4.737	4.995
CH16 str	4.822	4.872	5.042		
CH14 str	4.778	4.865	4.812		
CH15 str	4.946	4.804	4.782		
MH22 str	4.875	4.857	4.860	4.872	4.862
MH20 str	4.820	4.799	4.756	4.820	4.751
MH21 str	4.820	4.751	4.796	4.820	4.803
MCN def	0.946	0.968	1.034	0.952	0.996
CO ib1	1.153	1.208	1.242	1.111	1.201
CNC^{α} def	0.924	1.149	1.432	0.812	1.154
NH ib1	0.553	0.585	0.614	0.549	0.585
$C^{\alpha}CN$ def	1.018	1.164	1.256	0.955	1.156
CO ib2	1.276	1.163	1.107	1.222	1.063
CNM def	0.794	0.814	0.826	0.783	0.813
NH ib2	0.585	0.656	0.659	0.588	0.642
M1 sb	0.549	0.551	0.551	0.545	0.547
M1 ab1	0.521	0.519	0.519	0.521	0.519
M1 ab2	0.522	0.521	0.522	0.522	0.521
M1 rock1	0.649	0.652	0.656	0.647	0.653
M1 rock2	0.605	0.607	0.606	0.579	0.582
$NC^{\alpha}C$ def	1.020	1.043	1.882		
H^{α} b1	0.637	0.666	0.708		
H^{α} b2	0.697	0.736	0.744		
C^{β} b1	1.393	1.410	1.116		
C^{β} b2	1.109	1.134	0.956		
C^{β} sb	0.556	0.556	0.560		
C^{β} ab1	0.539	0.533	0.533		
C^{β} ab2	0.536	0.533	0.545		
C^{β} rock1	0.669	0.673	0.690		
C^{β} rock2	0.649	0.664	0.674		

TABLE 4 (continued)

	ALA5	ALA7E	ALA7A	GLY5	GLY7
M2 sb	0.607	0.602	0.601	0.607	0.606
M2 ab1	0.544	0.548	0.548	0.544	0.548
M2 ab2	0.535	0.540	0.541	0.535	0.541
M2 rock1	0.783	0.781	0.780	0.785	0.780
M2 rock2	0.796	0.792	0.791	0.771	0.765
CO ob1	0.777	0.803	0.825	0.766	0.802
NH ob1	0.220	0.243	0.293	0.205	0.250
CO ob2	0.802	0.790	0.787	0.789	0.780
NH ob2	0.234	0.255	0.303	0.165	0.219
MC tor	0.060	0.058	0.062	0.061	0.059
CN tor1	0.446	0.546	0.561	0.447	0.541
NC^{α} tor	0.385	0.544	0.724	0.250	0.530
$C^{\alpha}C$ tor	0.320	0.397	0.552	0.267	0.315
CN tor2	0.374	0.498	0.522	0.367	0.506
NM tor	0.050	0.054	0.055	0.050	0.053
$C^{\alpha}C^{\beta}$ tor	0.163	0.121	0.142		

[a]Units: stretches, mdyn $Å^{-1}$; bends and torsions, mdyn Å rad^{-2}.

angle increases. If we then look at f(CO ib), we see that this conclusion also seems to be borne out: for example, the value is lowest in ALA7A and GLY7 where the differences in the adjacent angles of CO ib2 are largest, 3.3° (ALA7A) and 2.0° (GLY7); that the ALA7A value is larger than the GLY7 may be a result of the larger opposite angle, 116° versus 114°. The bonded f(NH ob) in ALA7E and ALA7A is larger than the free, but in ALA5 the reverse is seen. That the free f(NH ob1) is quite different in the two C_7 structures shows a strong sensitivity to the conformation at the adjacent C^{α} atom, and probably accounts for the ALA5 results.

We noted in GLY5 and GLY7 the significant sizes of some interaction terms involving the NH stretches and attributed these to the C_5 and C_7 hydrogen bonds. In Ala dipeptide we find similarly large terms: the bonded f(NH str − NH ib) has the magnitudes −0.11 (ALA5), 0.11 (ALA7E) and 0.12 (ALA7A), whereas the free term is no larger in magnitude than 0.04; and f(NH str1 − CO str2) is −0.10 mdyn $Å^{-1}$ in ALA5 while f(NH str2 − CO str1) is −0.14 and −0.17 mdyn $Å^{-1}$ in ALA7E and ALA7A. The signs of these terms are again consistent with the C_5 and C_7 hydrogen bonds, and their relative values show that they increase in magnitude with the strength of the hydrogen bond.

Thus, as in Gly dipeptide, our results on the CONH force constants show the presence of the C_5 and C_7 hydrogen bonds in these Ala dipeptide conformations. We should mention that we have not computed hydrogen-bond force constants such as f(H···O str) and f(NH···O bend) [4] because these coordinates would be redundant in these structures. That is, displacements of the

TABLE 5

Normal modes of Ala dipeptides using scaled force constants

ν (cm^{-1})	I[a] (km mol^{-1})	Potential energy distribution > 10%
ALA5		
3471	59	NH str2(100)
3390	64	NH str1(100)
3022	4	MH1 str(84)
3016	1	CH15 str(77), CH16 str (19)
3000	7	MH22 str (72), MH21 str (15), MH20 str (14)
2985	15	CH14 str(41), CH16 str(32), $C^{\alpha}H^{\alpha}$ str(16)
2980	13	MH20 str(49), MH21 str(48)
2972	3	MH2 str(50), MH3 str(50)
2946	2	$C^{\alpha}H^{\alpha}$ str(81), CH16 str(12)
2907	34	MH20 str(35), MH21 str(35), MH22 str(28)
2904	2	MH2 str(42), MH3 str(41), MH1 str(16)
2901	14	CH14 str(49), CH16 str(35), CH15 str(16)
1698	14	CO str2(47), CO str1(34)
1668	445	CO str1(52), CO str2(32)
1557	173	NH ib2(49), CN str2(28)
1525	645	NH ib1(49), CN str1(25), NH ib2(12)
1476	2	M2 ab1(92)
1465	25	C^{β} ab1(92)
1459	31	C^{β} ab2(90)
1453	6	M2 ab2(95)
1446	9	M1 ab2(94)
1435	42	M1 ab1(90)
1412	1	M2 sb(102)
1372	42	M1 sb(87), MC str(11)
1368	12	C^{β} sb(99)
1347	137	H^{α} b2(28), $C^{\alpha}C$ str(16), M1 sb(12)
1303	34	H^{α} b1(74)
1276	9	CN str1(23), NH ib1(20), CN str2(14), CO ib1(11)
1229	65	H^{α} b2(40), CN str2(14)
1177	12	M2 rock1(28), NC^{α} str(25)
1158	5	M2 rock1(35), NC^{α} str(24)
1134	1	M2 rock2(89)
1100	6	$C^{\alpha}C^{\beta}$ str(35), C^{β} rock1(24)
1067	10	C^{β} rock1(20), H^{α} b2(14), C^{β} rock2(13), H^{α} b1(11)
1063	18	M1 rock2(68), CO ob1(15)
1031	9	NM str(52), C^{β} rock2(16)
1009	14	M1 rock1(45), $C^{\alpha}C^{\beta}$ str(12), CN str1(11)
959	20	MC str(34), C^{β} rock2(14)
898	8	$C^{\alpha}C^{\beta}$ str(22), NC^{α} str(13), C^{β} rock1(13)
852	5	$C^{\alpha}C$ str(17), M2 rock1(12), CN str2(10)
758	76	CO ob2(55)
693	85	NH ob1(32), CN tor1(23), CO ib2(15), NC^{α} tor(14)
683	68	NH ob1(39), CN tor1(25), NC^{α} tor(24), CO ob2(14)
639	31	CO ob1(66), M1 rock2(18)
609	26	CO ib1(26), CO ob1(13), CO ib2(12), MC str(12)
585	113	NH ob2(111), CN tor2(57)
501	17	CO ib1(28), MCN def(19), C^{α} CN def(13), C^{β} b2(11), NC^{α} C def(10)

TABLE 5 (continued)

ν (cm^{-1})	I[a] (km mol^{-1})	Potential energy distribution > 10%
398	12	C^{β} b1(30), NC^{α} C def(26)
350	25	MCN def(32), CNM def(24), CO ib2(18)
312	3	C^{β} b2(33), $C^{\alpha}C^{\beta}$ tor(23)
292	2	$C^{\alpha}C^{\beta}$ tor(62)
278	2	C^{β} b1(15), C^{β} b2(14), $C^{\alpha}C^{\beta}$ tor(13)
231	8	CNM def(26), CNC^{α} def(25), C^{α} CN def(24), MCN def(12)
185	1	MC tor(40), CN tor2(20)
169	1	MC tor(67), CN tor2(20), NC^{α} tor(12), CO ob2(10)
154	2	NM tor(85), NH ob2(10)
142	3	NM tor(49), NH ob1(25), $C^{\alpha}C$ tor(24), CN tor1(13), $NC^{\alpha}C$ def(11)
132	15	$C^{\alpha}C$ tor(30), NC^{α} tor(28), NH ob1(19), CN tor1(10)
110	12	CN tor1(24), C^{β} b1(23), CNC^{α} def(15), $C^{\alpha}CN$ def(11)
82	1	$C^{\alpha}C$ tor(71), NC^{α} tor(50)
ALA7E		
3414	22	NH str1(100)
3360	122	NH str2(100)
3024	2	MH1 str(85)
3010	5	$C^{\alpha}H^{\alpha}$ str(43), CH16 str(40)
2992	8	MH22 str(70), MH20 str(21)
2990	7	CH14 str(61), CH15 str(38)
2977	1	$C^{\alpha}H^{\alpha}$ str(49), CH16 str(32)
2971	3	MH2 str(49), MH3 str(44)
2965	20	MH20 str(49), MH21 str(47)
2907	15	CH15 str(47), CH16 str(26), CH14 str(25)
2906	1	MH3 str(45), MH2 str(38), MH1 str(15)
2896	31	MH21 str(45), MH20 str(29), MH22 str(24)
1704	222	CO str2(64), NH ib2(26)
1676	149	CO str1(70), NH ib1(15)
1587	416	NH ib2(59), CN str2(27), CO str2(21)
1534	405	NH ib1(60), CN str1(28), CO str1(14)
1478	3	M2 ab1(92)
1470	7	C^{α} ab2(68), C^{β} ab1(19)
1456	5	M2 ab2(94)
1453	9	C^{β} ab1(73), C^{β} ab2(19)
1445	11	M1 ab2(93)
1432	41	M1 ab1(90)
1412	2	M2 sb(99)
1379	9	C^{β} sb(103)
1372	34	M1 sb(99)
1353	40	H^{α} b2(29), $C^{\alpha}C$ str(22), H^{α} b1(16), CN str2(16)
1310	90	H^{α} b2(34), H^{α} b1(20), CN str1(18), CO ib1(10)
1279	78	H^{α} b1(28), CN str1(23), NH ib1(16)
1258	59	CN str2(31), H^{α} b2(20), H^{α} b1(16), NM str(13)
1172	2	M2 rock1(61)
1158	27	NC^{α} str(23), C^{β} rock2(19)
1134	1	M2 rock2(90)
1125	10	$C^{\alpha}C^{\beta}$ str(30), NC^{α} str(22), C^{β} rock1(11)

TABLE 5 (continued)

ν (cm^{-1})	I^a (km mol^{-1})	Potential energy distribution > 10%
ALA7E		
1067	27	M1 rock2(66), CO ob1(16)
1062	5	C^{β} rock1(19)
1045	9	NM str(32), M1 rock1(17), C^{β} rock2(16)
1005	3	M1 rock 1 (30), $C^{\alpha}C^{\beta}$ str(17), NM str(16)
938	6	MC str(37), $C^{\alpha}C^{\beta}$ str(14)
898	2	NC^{α} str(19), C^{β} rock2(19), CNC^{α} def(16), CN str1(13), C^{β} rock1(11)
851	8	$C^{\alpha}C$ str(18), $C^{\alpha}CN$ def(11), M2 rock1(11), C^{β} rock1(10)
790	89	CO ob2(53), NH ob2(19), C^{β} b1(11)
754	138	NH ob2(51), CN tor2(40)
676	25	CO ib2(23), $C^{\alpha}C$ str(13)
628	27	CO ob1(73), M1 rock2(18)
591	38	CO ib1(34), MC str(14), NH ob1(13), NC^{α} tor(12)
577	127	NH ob1(102), CN tor1(76), NC^{α} tor(67)
478	9	$C^{\alpha}CN$ def(24), $NC^{\alpha}C$ def(13), C^{β} b1(12)
420	20	MCN def(46), CO ib1(18), $NC^{\alpha}C$ def(12)
330	23	CO ib2(33), CNM def(30), $NC^{\alpha}C$ def(17)
321	3	C^{β} b2(29), C^{β} b1(27), CN tor1(14), $C^{\alpha}C$ str(11)
291	5	C^{β} b2(31), C^{β} b1(10)
261	2	$C^{\alpha}C^{\beta}$ tor(86)
214	4	$C^{\alpha}CN$ def(33), CNC^{α} def(26), CNM def(16), MCN def(14)
189	2	NH ob2(18), CNC^{α} def(15), NM tor(15), $NC^{\alpha}C$ def(11), CN tor2(10)
186	7	MC tor(20), $C^{\alpha}CN$ def(15), CN tor1(14), NC^{α} tor(12), CNC^{α} def(10)
170	1	MC tor(85), NC^{α} tor(16)
161	2	NM tor(88)
118	15	NC^{α} tor(148)
104	2	CN tor1(33), $C^{\alpha}C$ tor(29), C^{β} b1(24), NH ob1(16)
90	9	$C^{\alpha}C$ tor(13), CN tor2(45), NH ob2(13)
ALA7A		
3446	58	NH str1(100)
3334	191	NH str2(99)
3044	3	CH16 str(77), $C^{\alpha}H^{\alpha}$ str(13)
3026	2	MH1 str(85)
2996	4	$C^{\alpha}H^{\alpha}$ str(46), MH22 str(34)
2990	3	MH22 str(40), $C^{\alpha}H^{\alpha}$ str(38), MH21 str(11)
2976	12	CH14 str(52), CH15 str(46)
2971	2	MH3 str(53), MH2 str(48)
2966	21	MH21 str(51), MH20 str(48)
2906	17	CH15 str(50), CH14 str(39), CH16 str(10)
2905	1	MH2 str(46), MH3 str(39), MH1 str(14)
2897	35	MH20 str(45), MH21 str(31), MH22 str(24)
1699	232	CO str2(51), NH ib2(23), CO str1(14)
1682	166	CO str1(55), CO str2(19), NH ib1(15)
1594	363	NH ib2(59), CN str2(28), CO str2(18)

TABLE 5 (continued)

ν (cm^{-1})	I[a] (km mol^{-1})	Potential energy distribution > 10%
ALA7A		
1551	347	NH ib1(60), CN str1(27), CO str1(14)
1478	3	M2 ab1(92)
1471	6	C^{β} ab2(88)
1459	18	C^{β} ab1(87)
1456	5	M2 ab2(95)
1446	11	M1 ab2(94)
1432	36	M1 ab1(91)
1412	2	M2 sb(100)
1375	8	C^{β} sb(101)
1371	36	M1 sb(98)
1335	22	H^{α} b2(30), CN str2(13), H^{α} b1(12)
1325	73	H^{α} b1(26), CN str2(19), H^{α} b2(18), $C^{\alpha}C$ str(13)
1292	148	CN str1(37), CO ib1(16), MC str(12)
1274	34	H^{α} b1(42), H^{α} b2(40)
1171	2	M2 rock1(61)
1147	24	C^{β} rock2(24), NC^{α} str(18), NM str(14)
1134	1	M2 rock2(87)
1127	4	C^{β} rock1(28), $C^{\alpha}C^{\beta}$ str(16), $NC^{\alpha}C$ def(15)
1101	11	NM str(24), NC^{α} str(21), $C^{\alpha}C^{\beta}$ str(20)
1066	22	M1 rock2(71), CO ob1(16)
1032	12	C^{β} rock2(29), M1 rock1(26)
985	5	M1 rock1(22), NM str(12), MC str(12), $C^{\alpha}C^{\beta}$ str(11), C^{β} rock2(11)
929	14	C^{β} rock1(24), MC str(21), $C^{\alpha}C^{\beta}$ str(11), H^{α} b1(10)
892	2	CNC^{α} def(19), NC^{α} str(13), CN str1(13)
824	83	NH ob2(22), CO ib2(14)
809	141	NH ob2(51), CN tor2(19)
771	5	CO ob2(49), CN tor2(12), C^{β} b1(11)
682	3	$NC^{\alpha}C$ def(32), MC str(22), CNC^{α} def(14)
647	44	CO ob1(41), NH ob1(18), M1 rock2(11)
613	11	CO ob1(43), M1 rock2(10)
581	121	NH ob1(116), NC^{α} tor(95), CN tor1(81)
512	31	CO ib1(48), CO ib2(15), $NC^{\alpha}C$ def(12)
384	14	MCN def(42), C^{β} b1(14)
354	4	C^{β} b1(27), C^{β} b2(25), CO ib2(13)
310	15	CNM def(49), $NC^{\alpha}C$ def(23), CO ib2(18)
281	7	C^{β} b2(30), NH ob2(26), MCN def(15), C^{β} b1(13), CN tor2(13)
277	1	$C^{\alpha}C^{\beta}$ tor(98)
219	5	CNC^{α} def(66), MCN def(21), $C^{\alpha}CN$ def(15)
199	5	$C^{\alpha}CN$ def(47), NC^{α} tor(36), $NC^{\alpha}C$ def(22), CNM def(16)
181	0	MC tor(51), C^{β} b2(13), $C^{\alpha}C$ tor(12)
174	0	MC tor(51), $C^{\alpha}C$ tor(25), NC^{α} tor(22), C^{β} b1(16), CN tor1(14), C^{β} b2(12)
164	2	NM tor(99)
138	14	NC^{α} tor(135)
108	4	$C^{\alpha}C$ tor(87), CN tor1(37), C^{β} b1(19), NH ob1(14), CN tor2(13)
96	8	$C^{\alpha}C$ tor(69), CN tor2(53), NH ob2(14), NC^{α} tor(14)

[a]Infrared intensity.

coordinates NH str, NH ib, etc., also distort the NH···OC geometry and, therefore, their force constants and dipole derivatives implicitly contain contributions from the non-covalent intramolecular coordinates, these contributions of course accounting in part for the changes in the different conformers.

We turn next to the other groups, whose force constants are expected to be affected more by the conformation than by the hydrogen bond. As in Gly dipeptide, the largest variations are seen primarily in the diagonal and off-diagonal terms involving the C^{α} atom. Especially notable are the changes in the CNC^{α} deformation (def), NC^{α} torsion (tor), $NC^{\alpha}C$ def and C^{β} bend1 (b1) terms. The latter two diagonal terms seem to be inversely related to each other and to be correlated with the $NC^{\alpha}C$ angle. The high $f(CNC^{\alpha}$ def) in ALA7A may be due to the large CNC^{α} angle, and the increases in $f(H^{\alpha}$ b1) and $f(H^{\alpha}$ b2) from ALA5 to ALA7A mirror the decreases in the $C^{\alpha}H^{\alpha}$ bond length and $CC^{\alpha}H^{\alpha}$ angle. The force constants of the terminal methyl groups vary little. In the $C^{\beta}H_3$ group, however, there are significant changes in the CH str and C^{β} rock terms.

Using our results on the five Gly and Ala dipeptide conformations, we have plotted in Fig. 2 the scaled NH str, CO str, CN str and CH str diagonal force constants versus their respective equilibrium bond lengths. In each plot a roughly linear relationship can be discerned, at least over these ranges in bond lengths; over larger ranges more complex relationships may be justified [8, 9]. Accordingly, we fitted each set of points with a straight line, taking bond length as independent variable, and found the following slopes, in units of mdyn $Å^{-2}$ and with the linear correlation coefficient in parentheses: NH str, -78 (-0.96); CO str, -88 (-0.97); CN str, -37 (-0.97); and CH str, -35 (-0.94). In our previous ab initio study [10] of the variation of NH bond length and force constant with intermolecular hydrogen-bond geometry, we found a slope of about -100 mdyn $Å^{-2}$ for the unscaled STO-3G results; this value is the same as the NH str slope in Fig. 2 if we divide the latter by the scale factor of 0.80, thus confirming with an extended basis the trends given by our STO-3G results.

The slopes in Fig. 2 are quite interesting because they are very close to the respective diagonal cubic force constants, whose values averaged over all structures are (in mdyn $Å^{-2}$): NH str, -61; CO str, -89; CN str, -48; and CH str, -35. In the CN str plot, the points for CN str1 are clustered in the lower right corner; the points for CN str2 alone yield a slope of -58 mdyn $Å^{-2}$, compared to the average CN str2 cubic force constant of -52 mdyn $Å^{-2}$.

Although the expansion of the potential energy in terms of the internal coordinates shows that the diagonal second derivative of the potential with respect to each bond stretch should have a primary linear dependence on bond length with the cubic force constant as slope, the significance of these close agreements is not clear. It has been found that cubic stretching force constants [11, 12] and structures [13] are quite well reproduced at the SCF level with a medium-size basis set. It might be concluded, therefore, that the comparison

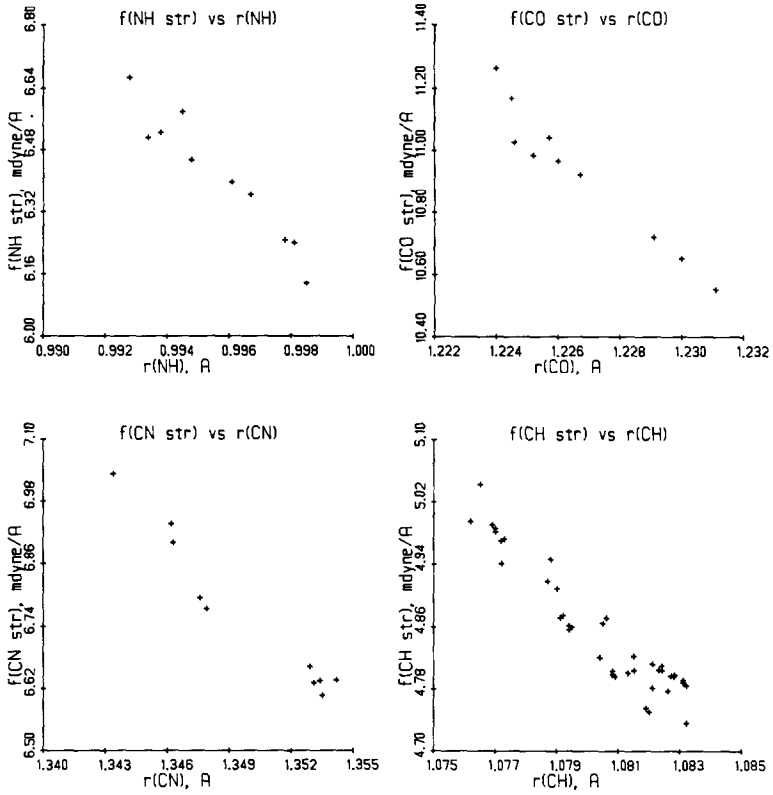

Fig. 2. Scaled NH str, CO str, CN str and CH str diagonal force constants plotted against their respective equilibrium bond lengths.

shows the slopes are reliable and that the scale factors are also, which suggests that this may be a way to derive scale factors ab initio, albeit with considerable effort. This implies that the effects of the quartic and off-diagonal cubic terms are not significant, and that the anharmonicities of the modes can be neglected, because the scale factors were chosen to fit observed frequencies.

We have also examined the force constant versus bond length correlations for NC^{α} str, $C^{\alpha}C$ str, MC str and NM str (where M represents a terminal methyl). The least-squares slopes are -15, -15, -12 and -20 mdyn $Å^{-2}$, respectively, compared with the average diagonal cubic force constants of -23, -22, -23 and -30 mdyn $Å^{-2}$. Because there are only five data points in each case and the MC str and NM str points are clustered in relatively small regions, these slopes are less meaningful. Similar plots for all carbon–carbon bonds (i.e. $C^{\alpha}C$, MC and $C^{\alpha}C^{\beta}$) or of all carbon–nitrogen single bonds (NC^{α} and NM) yield very scattered points with linear correlation coefficients of -0.48 and -0.79, respectively. Many other quantitative correlations, for example of an-

1698
1668
1557
1525
1347
1303
1276
1229
1177
1158
1134
1100
1067
1063
1031
1009
959
898
852
758

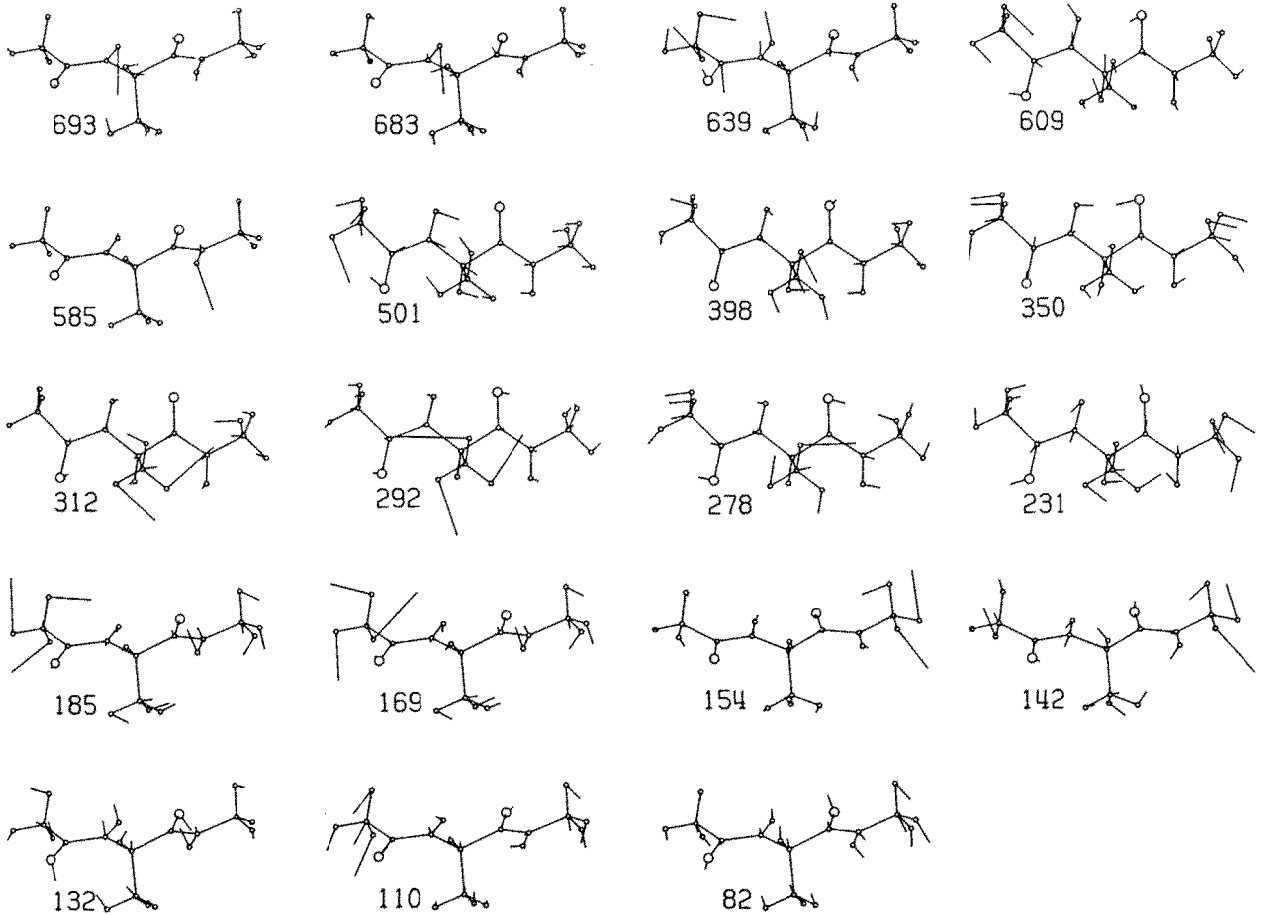

Fig. 3. Normal modes of ALA5, excluding XH stretches and CH_3 bends. Oxygen atoms are drawn disproportionately large. Calculated frequencies in cm^{-1} shown.

gle deformation force constants with various structural parameters, can be examined.

We turn next to the normal modes computed with the scaled force constants (Table 5). Figure 3 shows plots of the atomic displacements in the modes of ALA5, excluding the NH and CH stretches and the well-localized methyl symmetric and antisymmetric bends. Figures 4 and 5 show similar plots for most

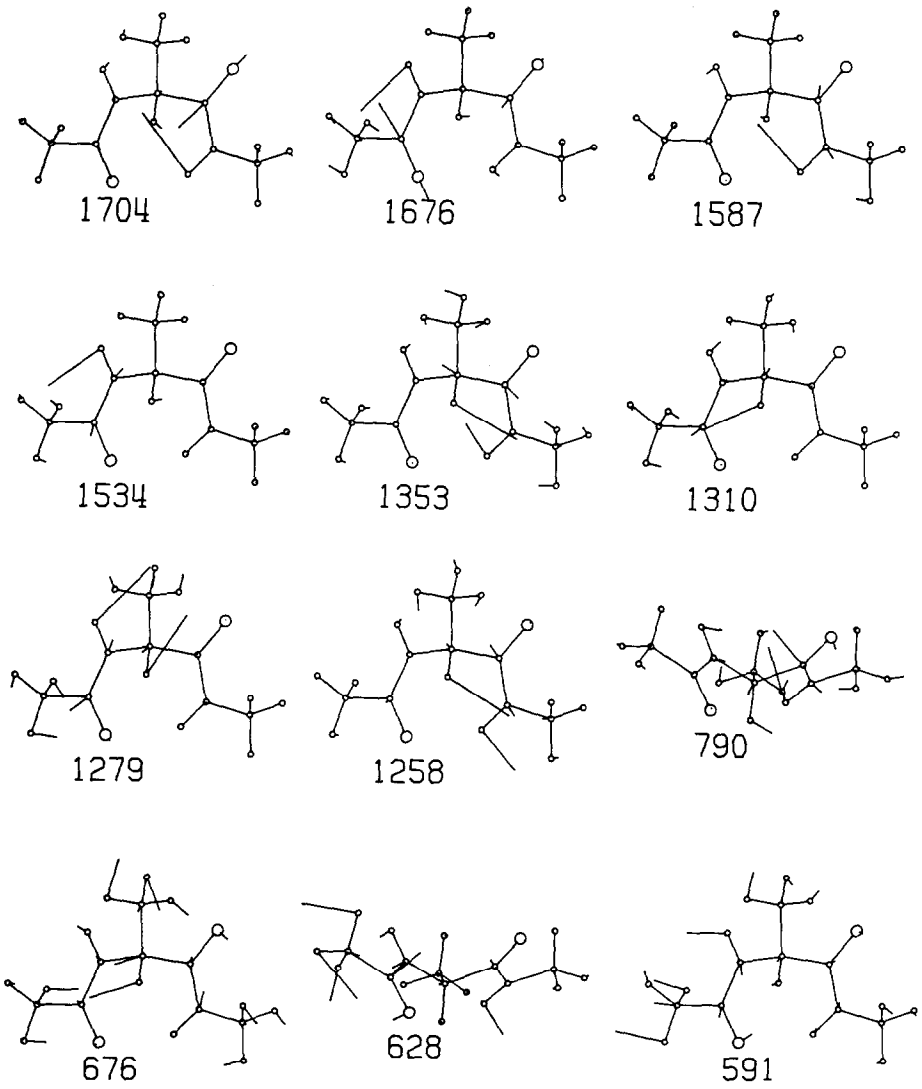

Fig. 4. Some normal modes of ALA7E. Oxygen atoms are drawn disproportionately large. Calculated frequencies in cm^{-1} shown.

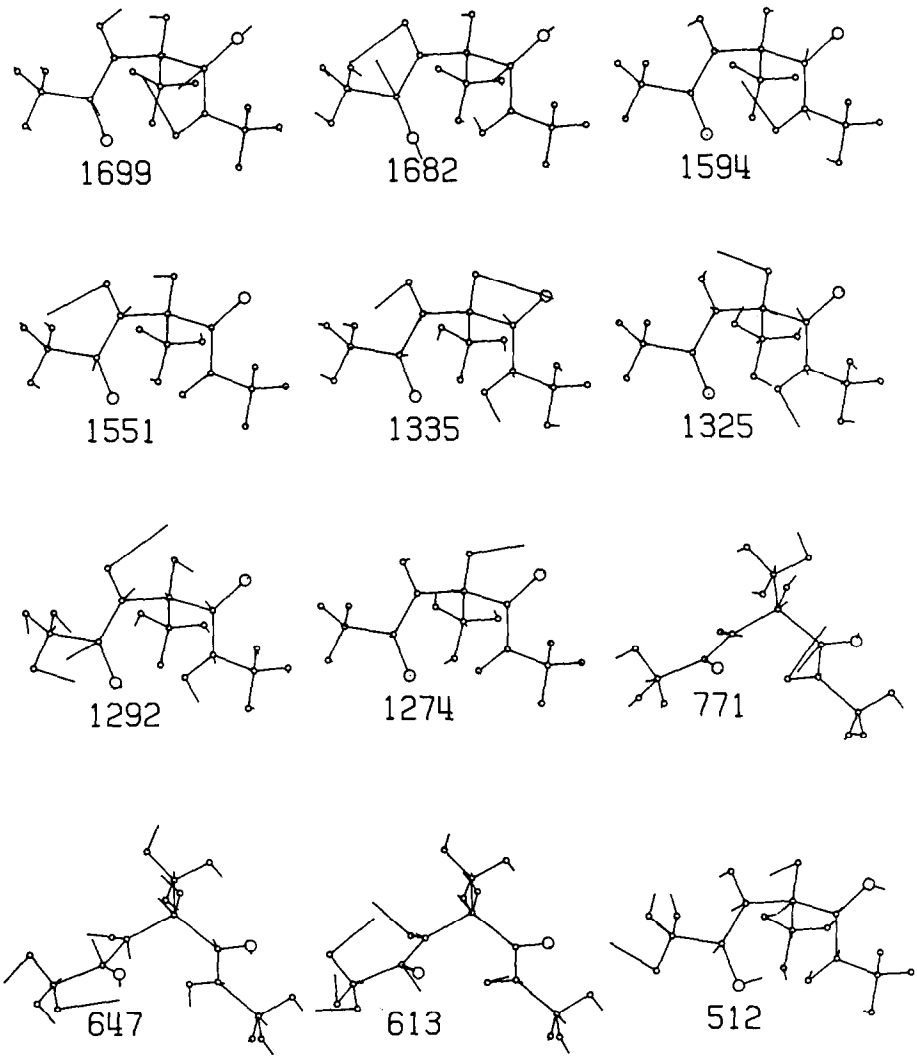

Fig. 5. Some normal modes of ALA7A. Oxygen atoms are drawn disproportionately large. Calculated frequencies in cm^{-1} shown.

of the amide modes of ALA7E and ALA7A, and include the H^{α} bends, which mix with amide **III** in the 1300 cm^{-1} region.

The NH stretches show clearly the effects of the C_5 and C_7 hydrogen bonds: the bonded NH str is substantially lower in frequency than the free, and the bonded NH str frequency is lowest in ALA7A. In ALA5 the bonded frequency (3390 cm^{-1}) is close to that in GLY5 (3400 cm^{-1}), but the free frequency is much higher (3471 cm^{-1} versus 3431 cm^{-1}). Whereas the free frequencies in GLY5 and GLY7 are nearly identical, the free frequencies in Ala dipeptide are

quite different, decreasing by 57 cm^{-1} from ALA5 to ALA7E. In the C_7 Ala conformations, the free NH group is adjacent to the $C^{\alpha}C^{\beta}H_3$ group and its stretching frequency seems to be affected by the conformational relationship of the two groups, as has been proposed previously [14].

The stretching frequencies of the terminal methyl groups are nearly identical to those of GLY5 or GLY7. The M2 stretches in the C_7 conformations are about 10 cm^{-1} lower than in ALA5. While the $C^{\beta}H_3$ symmetric stretch (ss) at 2901 cm^{-1} in ALA5 moves by only 6 cm^{-1} in the C_7 structures, the $C^{\beta}H_3$ antisymmetric stretches (as) and $C^{\alpha}H^{\alpha}$ str shift considerably with conformation. The $C^{\beta}H_3$ and $C^{\alpha}H^{\alpha}$ str are mixed to various extents because of near degeneracy. To remove the mixings and, thereby, obtain a clearer picture of how sensitive these stretches are to conformation, we have done normal-mode calculations with each group selectively deuterated. The $C^{\beta}H_3$ as modes in C^{α}-deuterated Ala dipeptide are at 3014 and 2979 cm^{-1} (ALA5), 2997 and 2990 cm^{-1} (ALA7E), and 3038 and 2977 cm^{-1} (ALA7A). The $C^{\alpha}H^{\alpha}$ stretches in Ala dipeptide with all three methyl groups deuterated are at 2955 (ALA5), 2991 (ALA7E) and 3000 cm^{-1} (ALA7A). Whilst the $C^{\beta}H_3$ frequencies are very reasonable when compared to data on L-alanine [15–17] and cyclo (D-Ala–L-Ala) [18], the $C^{\alpha}H^{\alpha}$ str may be somewhat high, indicating that the scale factors for the methyne and methyl stretches should be different. We see from these deuterium-isolated frequencies that the $C^{\alpha}H^{\alpha}$ str and $C^{\beta}H_3$ as, and particularly the separation of the two antisymmetric stretches, are very sensitive to conformation, as we concluded from our experimental analysis [18] of cyclo(D-Ala–L-Ala) in two crystalline forms. We note that in cyclo(D-Ala–L-Ala) the $C^{\beta}H_3$ as modes are well separated from the $C^{\alpha}H^{\alpha}$ str and hence, they do not mix, as was shown by normal mode calculations [18]. In cyclo-(D-Ala–L-Ala) we found the $C^{\alpha}H^{\alpha}$ str frequency to be higher when the $C^{\alpha}H^{\alpha}$ bond is more nearly equatorial to the ring (form **I**) than when the bond is more nearly axial (form **II**). The orientation of the $C^{\alpha}H^{\alpha}$ bond in ALA7A more closely resembles that in form **I** and its isolated frequency is indeed higher than in ALA7E where the $C^{\alpha}H^{\alpha}$ orientation is more similar to that in form **II**. We concluded [18] that the $C^{\alpha}H^{\alpha}$ str frequency correlated well with the adjacent dihedral angles; systematic calculations of $f(C^{\alpha}H^{\alpha}$ str) in Ala dipeptide in more conformations would be useful in deriving a quantitative correlation for the mode in *trans* peptides.

The amide **I**, which is mainly CO str and NH ib, and amide **II**, mainly CN str and NH ib, are seen in Table 5 and Figs. 3–5 to resemble closely the corresponding modes in GLY5 and GLY7. These modes are more localized in the C_7 structures than in ALA5, and the relative frequencies of the amide **I** and **II** pairs in ALA7E and ALA7A follow the order expected: the amide **I** involving mainly the hydrogen-bonded CO str1 is lower in frequency, and the amide **II** involving the bonded NH ib2 is higher in frequency.

We saw in GLY5 and GLY7 that CN str and NH ib are mixed with CH_2 wag

in the amide **III** modes around 1300 cm^{-1}. In Ala dipeptide, the amide **III** contains a H^{α} bend. The interaction force constants between H^{α} b1 or H^{α} b2 and CN str or NH ib are relatively small, $\leqslant 0.07$ in magnitude; therefore, the strong mixing is mainly due to kinetic coupling. In C^{α}-deuterated Ala dipeptide, the amide **III** modes are at 1321 and 1276 cm^{-1} (ALA5), 1322 and 1286 cm^{-1} (ALA7E), and 1327 and 1294 cm^{-1} (ALA7A); thus, when H^{α} b is excluded, the trend of the amide **III** frequency with ψ is in qualitative agreement with Lord's proposed relation [19]. By contrast, in *N*-deuterated Ala dipeptide, where the amide **III**′ frequencies are in the 900 cm^{-1} region, the H^{α} b modes are at 1315 and 1288 cm^{-1} (ALA5), 1314 and 1305 cm^{-1} (ALA7E), and 1317 and 1274 cm^{-1} (ALA7A). Thus, while the "pure" amide **III** varies over as much as 18 cm^{-1}, the "pure" H^{α} b varies over 31 cm^{-1}. Of course, the "pure" amide **III** is affected by hydrogen bonding as well as conformation, and these effects may be in opposite directions. Even so, it is clear that much of the conformational sensitivity of the modes around 1300 cm^{-1} in peptides seen here and in other work [4, 19] is due to the H^{α} b components. Also, in general, one should consider all amide and H^{α} b modes in this region when trying to correlate amide **III** frequencies with conformation. (We note that in cyclo(D-Ala–L-Ala), where the peptide units are *cis*, the H^{α} b modes are quite pure and we were able to ascribe their shifts in the two forms to conformational rather than hydrogen-bonding differences [18].)

The amide **V** modes, mainly NH ob and CN tor, show trends related to the C_5 and C_7 hydrogen bonds. While the free amide **V** remains at about 580 cm^{-1} in all three conformations, the bonded mode appears at $\sim$690 cm^{-1} in ALA5 (there being two modes with similar amide **V** character in this region), at 754 cm^{-1} in ALA7E, and at 809 cm^{-1} in ALA7A. Thus, the well-localized amide **V**, together with the NH str, shows the best-defined changes with hydrogen bonding. The modes involving CO ib and CO ob are more delocalized (Figs. 3–5) and are not readily relatable to hydrogen bonding. For instance, the 758 cm^{-1} mode in ALA5, which is mainly CO ob2, shifts to 790 cm^{-1} in ALA7E even though CO ob2 becomes free in the C_7 conformation. CO ob2 is adjacent to C^{α} and probably the conformational effects more than compensate for the change in hydrogen bonding.

DIPOLE-MOMENT DERIVATIVES AND INTENSITIES

Table 6 lists the dipole derivatives $\partial\vec{\mu}/\partial S_i$ with respect to the group coordinates of the peptide and side-chain groups, referred to local axes fixed within each group [1]; see Table 6 footnote for definitions of local axes. The derivatives of the terminal CH_3 groups are not shown; these are very nearly identical to those of GLY5 and GLY7, and where there are differences between GLY5 and GLY7 the same differences occur between the derivatives in C_5 and C_7 Ala dipeptide.

Looking first at the peptide groups, we see that the bonded NH str deriva-

TABLE 6

Dipole-moment derivatives $\partial\vec{\mu}/\partial S$ (in D Å^{-1} or D rad^{-1}) of Ala dipeptides with respect to group axes[a]

	$\partial\mu_x/\partial S$	$\partial\mu_y/\partial S$	$\partial\mu_z/\partial S$	$\lvert\partial\vec{\mu}/\partial S\rvert$	θ^b
C6 N7 O5					
NH str1	0.90	0.43	0.04	1.00	26
	0.32	0.40	0.03	0.51	51
	0.67	0.75	−0.09	1.01	48
CO str1	4.23	4.47	−0.01	6.15	47
	4.25	5.10	−0.14	6.64	50
	3.99	5.22	0.16	6.57	53
CN str1	−4.70	−0.20	0.11	4.71	−178
	−4.07	−0.22	−0.05	4.08	−177
	−3.74	−0.12	−0.09	3.74	−178
MC str	0.56	−0.17	−0.04	0.58	−17
	0.55	−0.25	0.04	0.60	−25
	0.59	−0.31	0.01	0.67	−28
NC^{α} str	1.69	−1.32	−0.41	2.19	−38
	1.96	−2.09	0.10	2.87	−47
	2.11	−2.52	0.21	3.29	−50
MCN def	−1.99	0.89	0.05	2.18	156
	−1.54	1.35	−0.20	2.06	139
	−1.69	1.31	0.20	2.15	142
CO ib1	−3.16	2.14	0.08	3.81	146
	−2.92	2.43	−0.34	3.81	140
	−2.86	2.68	0.24	3.93	137
CNC^{α} def	4.20	−1.38	−0.06	4.42	−18
	2.84	−3.08	0.23	4.20	−47
	2.79	−3.44	−0.16	4.43	−51
NH ib1	0.91	−0.37	0.14	0.99	−22
	0.53	−0.26	−0.01	0.59	−26
	0.50	−0.11	−0.05	0.52	−13
CO ob1	−0.09	0.01	0.80	0.81	174
	0.20	−0.02	1.52	1.54	−7
	−0.05	0.05	1.63	1.63	133
NH ob1	0.01	0.04	2.27	2.27	74
	−0.26	−0.13	1.03	1.07	−153
	0.18	0.03	0.77	0.79	9
MC tor	−0.00	−0.00	−0.17	0.17	−140
	0.02	0.01	−0.18	0.18	22
	−0.03	−0.01	−0.18	0.18	−164
CN tor1	0.22	−0.13	−3.47	3.48	−31
	−0.50	0.43	−3.39	3.45	139
	0.37	−0.46	−3.37	3.42	−51
NC^{α} tor	0.17	−0.07	−3.36	3.36	−24
	−0.19	0.81	−4.90	4.97	103
	0.13	−1.03	−5.19	5.29	−83

TABLE 6 (continued)

	$\partial\mu_x/\partial S$	$\partial\mu_y/\partial S$	$\partial\mu_z/\partial S$	$\lvert\partial\vec{\mu}/\partial S\rvert$	θ^b
C12 N17 O13					
NH str2	0.62	0.72	−0.02	0.95	50
	0.19	1.40	−0.37	1.46	82
	0.14	1.85	0.47	1.91	86
CO str2	4.19	4.79	0.23	6.37	49
	4.47	4.68	−0.37	6.48	46
	4.45	4.96	0.12	6.67	48
CN str2	−4.42	−0.40	0.09	4.44	−175
	−3.87	−0.30	0.21	3.89	−176
	−3.52	−0.43	−0.28	3.56	−173
$C^{\alpha}C$ str	0.30	0.16	−0.19	0.39	28
	0.62	−0.53	0.43	0.92	−41
	0.97	−0.87	−0.22	1.32	−42
NM str	1.56	−2.74	0.08	3.15	−60
	1.27	−2.72	0.08	3.00	−65
	1.21	−2.71	−0.06	2.97	−66
$C^{\alpha}CN$ def	1.08	−1.42	−0.02	1.78	−53
	0.40	−2.96	0.34	3.01	−82
	0.20	−3.07	−0.31	3.09	−86
CO ib2	−3.23	2.41	0.05	4.03	143
	−2.58	2.40	−0.05	3.53	137
	−2.21	2.30	−0.11	3.19	134
CNM def	0.73	0.32	0.01	0.79	24
	0.99	0.84	−0.06	1.30	40
	1.15	0.87	0.02	1.44	37
NH ib2	0.59	−0.12	−0.03	0.61	−12
	0.73	−0.45	0.27	0.90	−32
	0.66	−0.54	−0.18	0.87	−39
CO ob2	−0.05	−0.02	0.85	0.85	−160
	0.06	−0.21	−0.33	0.39	−75
	−0.08	0.17	−0.38	0.43	115
NH ob2	−0.00	0.09	2.24	2.24	91
	0.20	0.08	2.66	2.67	22
	−0.05	−0.05	2.70	2.70	−139
$C^{\alpha}C$ tor	0.11	−0.15	3.38	3.39	−52
	−0.01	−0.29	4.37	4.38	−91
	0.11	0.51	4.32	4.35	78
CN tor2	−0.11	0.08	−0.06	0.15	143
	0.34	−0.38	−0.33	0.61	−48
	−0.19	0.36	−0.41	0.58	118
NM tor	0.01	−0.00	0.19	0.19	−6
	−0.05	−0.03	0.20	0.21	−152
	0.03	0.02	0.20	0.20	31
C11 C9 H16					
$C^{\alpha}C^{\beta}$ str	−0.65	0.10	−0.15	0.68	171
	−0.72	−0.18	0.07	0.75	−166
	−0.69	−0.08	0.02	0.69	−174

TABLE 6 (continued)

	$\partial\mu_x/\partial S$	$\partial\mu_y/\partial S$	$\partial\mu_z/\partial S$	$\lvert\partial\vec{\mu}/\partial S\rvert$	θ^b
C11C9H16					
$C^\alpha H^\alpha$ str	−0.18	0.18	−0.26	0.36	136
	0.29	0.21	−0.14	0.39	36
	0.15	0.05	0.04	0.17	20
CH16 str	0.34	0.18	0.03	0.39	28
	−0.00	0.01	0.07	0.07	100
	−0.04	−0.29	−0.06	0.30	−98
CH14 str	0.27	−0.08	−0.16	0.67	−16
	0.33	−0.17	−0.26	0.45	−28
	0.25	−0.31	−0.36	0.54	−51
CH15 str	0.14	0.07	0.09	0.18	26
	0.36	−0.32	0.39	0.62	−42
	0.42	−0.24	0.44	0.65	−30
$NC^\alpha C$ def	0.04	0.45	−2.79	2.82	86
	−0.05	0.51	−2.95	3.00	96
	−0.08	0.88	4.28	4.37	95
H^α b1	−0.01	−0.05	−0.0	0.05	−102
	0.00	−0.11	−1.39	1.39	−88
	0.15	−0.19	1.49	1.51	−51
H^α b2	−0.90	−0.62	0.13	1.10	−146
	−0.45	0.97	0.08	1.07	115
	1.18	−0.38	0.15	1.25	−18
C^β b1	0.27	−0.05	−3.93	3.94	−11
	0.78	−0.41	2.34	2.50	−28
	0.43	−0.68	0.59	0.99	−58
C^β b2	0.54	0.24	0.36	0.69	24
	0.64	−1.39	0.35	1.56	−65
	−0.83	0.44	0.10	0.95	152
C^β sb	0.37	−0.02	−0.12	0.39	−2
	0.36	0.01	0.04	0.36	2
	0.38	−0.07	−0.03	0.39	−10
C^β ab1	0.09	−0.40	−0.01	0.41	−77
	0.04	−0.36	0.04	0.36	−84
	−0.03	−0.42	0.03	0.42	−95
C^β ab2	−0.02	−0.02	−0.37	0.37	−130
	−0.01	0.08	−0.37	0.37	100
	0.07	−0.04	−0.44	0.45	−31
C^β rock1	0.05	0.10	−0.13	0.17	62
	−0.18	0.18	−0.04	0.25	135
	−0.28	0.37	0.10	0.48	127
C^β rock2	0.14	0.13	−0.63	0.65	42
	−0.06	0.09	−0.34	0.36	122
	−0.07	−0.05	−0.40	0.41	−143
$C^\alpha C^\beta$ tor	0.01	−0.10	−0.06	0.11	−82
	0.04	−0.12	0.05	0.13	−72
	−0.02	0.13	0.14	0.20	101

[a]Local axes of group A B C are defined as: $\hat{x}$ = AB, $\hat{z}$ = AC×AB. Entries are for ALA5 (first line), ALA7E (second line), and ALA7A (third line). [b]Angle from $\hat{x}$ in the x-y plane, in degrees.

tives are as expected larger than the free. The difference is small in ALA5, probably because of the conformational effects on the NH str1 derivative, as evidenced by its values in ALA7E and ALA7A. The bonded derivative is largest in ALA7A, consistent with the NH···O geometries. From the directions, we see that while the free NH str derivatives are oriented at about 50° in the local x–y plane, the bonded derivatives are in each structure rotated further toward the respective oxygen atom. This was also seen in GLY5 and GLY7 and is due to the modulation of the H···O distance during displacement of a bonded NH str, resulting in a contribution from the H···O str derivative [10]. The CO str shows only slight increases on hydrogen bonding, and all the CO str derivatives are very close in magnitude and direction. The CN str derivatives are all nearly parallel to the CN bond and the C_5 (ALA5 and GLY5) derivatives are larger than the C_7. The NH and CO bend derivatives all reflect the C_5 or C_7 hydrogen bond, being larger when bonded. The NH ob1, adjacent to C^α, shows the strongest conformational dependence, as seen in its values in ALA7E and ALA7A. The CN tor1 is large and nearly the same in all conformations but the CN tor2 is very small.

Turning to the side-chain derivatives, there are significant differences among the conformations, except for the $C^\alpha C^\beta$ str and the $C^\beta H_3$ symmetric and antisymmetric bends (C^β sb and C^β ab). Drastic changes are seen in the $NC^\alpha C$ def and H^α and C^β bends. The $NC^\alpha C$ def, for example, is large in ALA5 and ALA7E and oriented almost perpendicular to the $H^\alpha C^\alpha C^\beta$ plane and toward N_7; in ALA7A, however, it is much larger in magnitude and oriented nearly in the opposite direction. The changes in the derivatives at the C^α atom show that these $\partial\vec{\mu}/\partial S_i$ are not transferable when the ϕ and ψ angles vary significantly. In these cases, the group moment model [20, 21] is not reliable in computing IR intensities of modes that have an appreciable contribution from the coordinates at C^α. It is clear, however, that for amides **I** and **II**, at least, the group moment model is applicable to a first approximation. It would also be interesting to see if other empirical models for calculating IR intensities [22] can reproduce such changes in $\partial\vec{\mu}/\partial S_i$ with conformation.

The IR intensities are given in Table 5. The NH str and amides **I**, **II** and **V** are generally the most intense modes. In each structure the bonded NH str and NH ob modes are stronger than the free (in ALA5 the NH ob1 intensity is distributed into two modes around 690 cm^{-1}), but the amides **I** and **II** do not show such clear-cut differences with hydrogen bonding. We find, as in Gly dipeptide, a smaller total intensity for the amide **I** pair than for the amide **II** pair, and that the most intense mode in each conformer is an amide **II**; these results are contrary to expectation and we suggested [1] that they could be due to deficiencies in both the dipole derivatives and the force fields. In our previous calculations [21] of the dipole derivatives in *N*-methylacetamide (NMA), we found that the 3-21G basis yields more accurate dipole moments and derivatives than the larger 4-31G and 6-31G bases. Using the 3-21G $\partial\vec{\mu}/$

∂S_i for the CONH group in NMA, we computed the amide **I** and **II** intensities in ALA7E (these modes being most localized in this struture). The results for the four modes are 211, 100, 285 and 322 km mol^{-1}, in descending order in frequency. The amide **II** pair is significantly reduced in intensity and the ratio of total intensities A_I/A_{II} increases from 0.45 to 0.51. We had concluded [21] that this ratio is improved if the amide **I** has more CN str and less NH ib contribution. One way this can be readily effected is by reducing the interaction terms f(CO str–CN str) from 1.36 and 1.30 mdyn $Å^{-1}$ in ALA7E to 0.50 mdyn $Å^{-1}$ which is the value assumed in the empirical polyglycine **I** force field [4]. Upon introducing these changes, the amide **I** and **II** frequencies in ALA7E shift about 20–30 cm^{-1} to 1736, 1712, 1609 and 1554 cm^{-1}, and the intensities, given by the NMA dipole derivatives, become 306, 151, 282 and 209 km mol^{-1}. The strongest band becomes an amide **I** and the ratio A_I/A_{II} increases to 0.93. Thus, the amide **I** and **II** intensities and intensity ratio are very sensitive to the dipole derivatives and force constants of the peptide groups. It is likely, then, that the scale factors for the force constants can be improved; in particular, f(CO str–CN str) may require a separate scale factor in view of its large magnitude [23]. It may also be necessary to scale the dipole derivatives or to recompute the $\partial\vec{\mu}/\partial S_i$ with the 3-21G basis set.

COMPARISON WITH EXPERIMENT

The C_5 and C_7 structures have been proposed in numerous IR studies of Ala dipeptide in solution [14, 24–30] and in argon matrix [31]; the IR spectrum of crystalline Ala dipeptide in the 700–300 cm^{-1} region [32] and the Raman spectra in H_2O and D_2O solution [33] have also been reported. Doubt has been raised [27, 30] about the earlier IR work on dipeptides in dilute carbon tetrachloride solution, in which the presence of C_7 conformers was inferred from the NH str region. Nevertheless, studies with various model compounds have shown that the C_7 hydrogen-bonded NH str is in the 3350 cm^{-1} region, whereas the C_5 bonded NH str is near 3420 cm^{-1}, and that the free NH str is found above 3440 cm^{-1} [25–27, 30, 31, 34]; an NH str band due to self-associated species may also appear near 3350 cm^{-1} [34].

In Table 7 we compare our calculations with the IR NH str and amide **I** and **II** frequencies observed in Ala dipeptide in argon matrix [31]. Because the number of observed bands evidently shows that more than one conformation is present, we have considered four different mixtures of the C_5, C_7^{eq}, and C_7^{ax} forms. (Properly, we should also have considered a C_7^{eq} form in the comparison [1] of our Gly dipeptide results with spectral data, but we did not do calculations on this conformation.) Of course, the comparison can only be suggestive because the actual conformations present in the matrix are not likely to correspond precisely to those used in our calculations, and there may be other conformers present, such as open non-hydrogen-bonded forms [3, 27, 30].

TABLE 7

Comparison of observed and calculated frequencies (in cm^{-1})

Obs.[a]	A[b]		B		C		D		
	ALA5	ALA7E	ALA5	ALA7A	ALA7E	ALA7A	ALA5	ALA7E	ALA7A
NH str									
3484w	3471 (59)		3471				3471		
3476w				3446 (58)		3446			3446
3465m		3414 (22)			3414			3414	
3413s	3390 (64)		3390		3360		3390	3360	
3350s		3360 (122)		3334 (191)		3334			3334
Amide I									
1705s		1704 (222)		1699 (232)	1704	1699		1704	1699
	1698 (14)		1698				1698		
1688m		1676 (149)		1682 (166)		1682		1676	1682
1680m	1668 (445)		1668		1676		1668		
Amide II									
1550s		1587 (416)		1594 (363)	1587	1594		1587	1594
1513sh	1557 (173)		1557				1557		
1508m		1534 (405)		1551 (347)		1551			1551
1496m	1525 (645)		1525		1534		1525	1534	

[a]Infrared bands in argon matrix [30]. [b]A–D are calculated frequencies combined in various sets. IR intensities (in km mol^{-1}) are given in parentheses.

From Table 7, we see that all the observed bands can be more or less satisfactorily explained by assuming a mixture of either two or three forms. Only the NH str region, it seems, requires a mixture of three conformers, unless one of the bands above 3460 cm^{-1} is attributed to a splitting due to interaction between nearby (but not adjacent) molecules in the matrix [31]. The amide **II** frequencies seem to require a C_5 form, in which case the $C_7^{eq} + C_7^{ax}$ mixture

is not indicated. For the other two binary mixtures, the amide **I** and **II** frequencies are slightly more satisfactorily fitted by $C_5 + C_7^{eq}$ than by $C_5 + C_7^{ax}$, as measured by the average errors: 8 cm^{-1} in both sets for amide **I**, and 34 versus 40 cm^{-1} for amide **II**. Thus, even though our assignments of the amide **I** and **II** bands disagree in detail with those of Grenie et al. [31], our results do support their conclusion that C_5 and C_7 structures are both present in the matrix-isolated sample.

Our results on the NH str modes are relevant to the problem of distinguishing C_7^{eq} structures from C_7^{ax}. It has been supposed that the free NH str in C_5 and C_7^{ax} structures coincide, whereas that in the C_7^{eq} form is lowered in frequency by perturbation from the $C^{\alpha}C^{\beta}$ group [14, 26, 29]. The free NH str in ALA7E is indeed considerably lowered in frequency, but although we found identical free NH str frequencies in GLY5 and GLY7 (GLY7 being the C_7^{ax} form), this is not the case in ALA5 and ALA7A. From the spectra of model compounds which are expected to form C_7 structures only of the axial or equatorial type [25, 26], it was concluded that the NH str free-bonded shift is larger in C_7^{eq} (about 135 versus 77 cm^{-1}), thus implying a stronger hydrogen bond in C_7^{eq}. The ab initio geometries [3] and our results on frequencies and dipole-moment derivatives indicate that the hydrogen bond is strongest in ALA7A, and that the bonded NH str frequency in ALA7A is lower than in ALA7E. This seeming disagreement with the observations may be because the hydrogen-bond geometries in the model compounds are constrained by the various substitutions to be different from the ab initio geometries in Ala dipeptide. We note, for example, that the H···O distance in GLY7 is 2.06 Å, whereas that in ALA7A is 1.94 Å.

CONCLUSIONS

We have followed up our previous calculations of the force field of Gly dipeptide with similar studies of Ala dipeptide. Our results on these five dipeptide structures, together with the work of Schäfer and coworkers [2, 3], provide a guide to the variations with conformation and hydrogen bonding of geometry, force constants, normal modes and dipole moment derivatives in peptides. These results should help in interpreting spectral data and in correlating spectra with structure. They should also help in developing and testing force fields for normal mode and molecular mechanics calculations of peptides.

ACKNOWLEDGEMENT

This research was supported by NSF grants DMB-8517812 and DMR-8806975. We thank The University of Michigan Computing Center for a generous special allocation of computing funds.

REFERENCES

1 T.C. Cheam and S. Krimm, J. Mol. Struct., 193 (1989) 1.
2 L. Schäfer, C. Van Alsenoy and J.N. Scarsdale, J. Chem. Phys., 76 (1982) 1439.
3 J.N. Scarsdale, C. Van Alsenoy, V.J. Klimkowski, L. Schäfer and F.A. Momany, J. Am. Chem. Soc., 105 (1983) 3438.
4 S. Krimm and J. Bandekar, Adv. Protein Chem., 38 (1986) 181.
5 IUPAC-IUB Commission on Biochemical Nomenclature, Biochemistry, 9 (1970) 3471.
6 P. Pulay, G. Fogarasi, F. Pang and J.E. Boggs, J. Am. Chem. Soc., 101 (1979) 2550.
7 G. Fogarasi and A. Balázs, J. Mol. Struct. (Theochem), 133 (1985) 105.
8 C.W. Bock, M. Trachtman and P. George, J. Comput. Chem., 2 (1981) 30.
9 D.M. Byler, H. Susi and W.C. Damert, Spectrochim. Acta, Part A, 43 (1987) 861.
10 T.C. Cheam and S. Krimm, J. Mol. Struct., 146 (1986) 175.
11 H.B. Schlegel, S. Wolfe and F. Bernardi, J. Chem. Phys., 63 (1975) 3632.
12 P. Pulay, J.G. Lee and J.E. Boggs, J. Chem. Phys., 79 (1983) 3382.
13 W.J. Hehre, L. Radom, P.v.R. Schleyer and J.A. Pople, Ab Initio Molecular Orbital Theory, Wiley, New York, 1986.
14 M. Marraud, J. Néel, M. Avignon and P.V. Huong, J. Chim. Phys., 67 (1970) 959.
15 D.M. Byler and H. Susi, Spectrochim. Acta, Part A, 35 (1979) 1365.
16 H. Susi and D.M. Byler, J. Mol. Struct., 63 (1980) 1.
17 M. Diem, P.L. Polavarapu, M. Oboodi and L.A. Nafie, J. Am. Chem. Soc., 104 (1982) 3329.
18 T.C. Cheam and S. Krimm, Spectrochim. Acta, Part A, 44 (1988) 185.
19 R.C. Lord, Appl. Spectrosc., 31 (1977) 187.
20 R.G. Snyder, J. Chem. Phys., 42 (1965) 1744.
21 T.C. Cheam and S. Krimm, J. Chem. Phys., 82 (1985) 1631.
22 W. Person and G. Zerbi (Eds.), Vibrational Intensities in Infrared and Raman Spectroscopy, Elsevier, Amsterdam, 1982.
23 P. Pulay, G. Fogarasi and J.E. Boggs, J. Chem. Phys., 74 (1981) 3999.
24 M. Tsuboi, T. Shimanouchi and S. Mizushima, J. Am. Chem. Soc., 81 (1959) 1406.
25 M. Avignon, P.V. Huong, J. Lascombe, M. Marraud and J. Néel, Biopolymers, 8 (1969) 69.
26 J. Néel, Pure Appl. Chem., 31 (1972) 201.
27 F.R. Maxfield, S.J. Leach, E.R. Stimson, S.P. Powers and H.A. Scheraga, Biopolymers, 18 (1979) 2507.
28 J. Smolíková, J. Pospíšek and K. Bláha, Coll. Czech. Chem. Commun., 46 (1981) 772.
29 I.M. Ginzburg, J. Gen. Chem., 52 (1982) 1445.
30 C.I. Jose, A.A. Belhekar and M.S. Agashe, Biopolymers, 26 (1987) 1315.
31 Y. Grenie, M. Avignon and C. Garrigou-Lagrange, J. Mol. Struct., 24 (1975) 293.
32 Y. Koyama, T. Shimanouchi, M. Sato and T. Tatsuno, Biopolymers, 10 (1971) 1059.
33 M. Avignon, C. Garrigou-Lagrange and P. Bothorel, Biopolymers, 12 (1973) 1651.
34 C.P. Rao, P. Balaram and C.N.R. Rao, Biopolymers, 22 (1983) 2091.